Accepted for publication in The Astrophysical Journal
Preprint typeset using LaTeX style emulateapj v. 5/2/11

ON THE RELATIVE SIZES OF PLANETS WITHIN *KEPLER* MULTIPLE CANDIDATE SYSTEMS

David R. Ciardi[1], Daniel C. Fabrycky[2], Eric B. Ford[3], T. N. Gautier III[4], Steve B. Howell[5], Jack J. Lissauer[5], Darin Ragozzine[3], Jason F. Rowe[5]

Accepted for publication in The Astrophysical Journal

ABSTRACT

We present a study of the relative sizes of planets within the multiple candidate systems discovered with the *Kepler* mission. We have compared the size of each planet to the size of every other planet within a given planetary system after correcting the sample for detection and geometric biases. We find that for planet-pairs for which one or both objects is approximately Neptune-sized or larger, the larger planet is most often the planet with the longer period. No such size–location correlation is seen for pairs of planets when both planets are smaller than Neptune. Specifically, if at least one planet in a planet-pair has a radius of $\gtrsim 3R_\oplus$, $68 \pm 6\%$ of the planet pairs have the inner planet smaller than the outer planet, while no preferred sequential ordering of the planets is observed if both planets in a pair are smaller than $\lesssim 3R_\oplus$.

Subject headings: planetary systems

1. INTRODUCTION

Approximately 20% of the planetary candidate systems discovered thus far by *Kepler* (Borucki et al. 2010) have been identified as having multiple transiting candidate planets (Batalha et al. 2012). As *Kepler* continues its mission, the number of multiple planet systems is likely to grow - not only because the total number of systems known to host planets will increase, but also because previously identified "single"-candidate systems may be found to have additional planets not previously detected. For example, 96 (11%) of the "single" candidate systems from the Borucki et al. (2011) *Kepler* Object of Interest (KOI) list are now listed on the Batalha et al. (2012) KOI list as having multiple planetary candidates. Thus, understanding planets in multiple systems is not only important for placing into context our own Solar System (the best studied planetary system), but multiple planetary systems may turn out to be the rule rather than the exception.

Typical detailed confirmation of individual planetary systems takes a concerted ground-based observational and modeling effort to rule out false positives caused by blends (e.g., Batalha et al. 2011; Torres et al. 2011). However, the multiple candidate systems provide additional information that can be used to confirm planets directly via transit timing variations (Steffen et al. 2012a; Fabrycky et al. 2012a) or via statistical arguments that multiple transiting systems discovered by *Kepler* are almost all true planetary systems (Latham et al. 2011; Lissauer et al. 2011b, 2012). Indeed, based upon orbital stability arguments, $\approx 96\%$ of the pairs within multiple candidate systems are most likely real planets around the same star (Fabrycky et al. 2012b).

ciardi@ipac.caltech.edu
[1] NASA Exoplanet Science Institute/Caltech Pasadena, CA 91125 USA
[2] UCO/Lick Observatory, U. of California, Santa Cruz, CA, USA
[3] Dept. of Astronomy, University of Florida, Gainesville, FL, USA
[4] Jet Propulsion Laboratory, Pasadena, CA, USA
[5] NASA Ames Research Center, Mountain View, CA USA

The higher statistical likelihood that candidates in multiple systems are true planetary systems has enabled studies of the properties of planetary systems with a lower level of false positive contamination than would be expected if all transiting systems were studied. The overall false positive rate within the *Kepler* candidate sample has been estimated to be $10 - 35\%$ (e.g., Morton & Johnson 2011; Santerne et al. 2012), but in comparison, the overall false positive rates among the multiple transiting systems is expected to be $\lesssim 1\%$ (Lissauer et al. 2012).

The multiple candidate systems also provide another level of certainty to the studies of planetary systems. The quality of knowledge of planetary characteristics for individual planets often is dependent upon the quality of knowledge of the host stellar characteristics. For example, planetary radii uncertainties for transiting planets are dominated by the uncertainties in the stellar radii (transit depth $\propto (R_p/R_\star)^2$), and changes in our understanding of the stellar radius can greatly alter our understanding of the radii of individual planets (e.g., Muirhead et al. 2012). By studying the *relative* properties of planets within multiple systems, systematic uncertainties associated with the stellar properties are minimized,

Understanding the relative sizes and, hence, the relative bulk compositions and structures of the planets within a system can yield clues on the formation, migration, and evolution of planets within an individual system and on planetary systems as a whole (e.g., Raymond et al. 2012). Within our Solar System, the distribution of the unique pair-wise radii ratios for each planet compared to the planets in orbits exterior to its orbit (e.g., Mercury-Venus, Mercury-Earth, ... Mercury-Neptune, Venus-Earth, Venus-Mars, ... etc.) is dominated by ratios less than unity (i.e., the inner planets are smaller than the outer planets). For the 8 planets in the Solar System, 20 of the 28 (70%) unique radii ratios are < 1, but only 3 out of 7 (42%) of neighboring pairs display this sequential size hierarchy. If only the terrestrial planets are considered (Mercury, Venus, Earth,

Mars), the fraction is 2/3 with only Mars being smaller than its inner companions.

How the planets sizes are ordered and distributed is likely a direct result of the how the planets formed and evolved. For example, Mars, being the only terrestrial planet in our Solar System that does not follow the sequential planet size distribution, may be a direct result of the formation and migration of Jupiter, inwards and then back outwards leaving a truncated and depleted inner disk out of which Mars was formed (Walsh et al. 2011).

Lissauer et al. (2011b) noted, for adjacent planets within the *Kepler* multiple-candidate systems, that the distribution of radii ratios for adjacent planets is symmetrically centered around unity, but hints of a planetary size hierarchy can be seen in multi-planet systems discovered by Kepler. *Kepler*-11, which has 6 transiting planets (Lissauer et al. 2011a) with the smallest planets residing preferentially inside the orbits of larger planets. *Kepler*-11 displays an anti-correlation between the mean density of the planets and the semi-major axis distance from the host star; i.e., the larger and lower density planets are located further out than the smaller and denser planets, possibly indicative of the formation and/or evolution of the planetary system (Migaszewski et al. 2012). *Kepler*-47, the only known circumbinary multiple planet system, also displays a size hierarchy with the inner planet ($\sim 3R_\oplus$) being smaller than the outer planet ($\sim 4.6R_\oplus$; Orosz et al. 2012). Yet, in *Kepler*-20 (a 5-planet system), the relative sizes of the planets do not appear to correlate with the orbital periods of the planets (Gautier et al. 2012; Fressin et al. 2012). But these are only three systems. Is there an overall correlation of planetary size with orbital period?

Here we explore the *relative* sizes of the planetary radii for all planet pairs within the multiple candidate systems discovered thus far by *Kepler* (Batalha et al. 2012). In this work, we refer to the Kepler candidates as "planets" though the majority have not been formally validated or confirmed as planets; as discussed above, candidates in multiple candidate systems are statistically more likely to be true planetary systems (Latham et al. 2011; Lissauer et al. 2011b, 2012). We seek to characterize the planetary size hierarchy, as a function of the number of planets detected in the systems and the properties of the stellar hosts, and explore if the size hierarchy seen within the inner Solar System also occurs in the *Kepler* multiple-candidate sample.

2. THE SAMPLE

The sample used here is based upon the 2012 KOI candidate list published by Batalha et al. (2012); a full description of the KOI list, the vetting that list underwent, and the characteristics of the sample set as a whole are described in the catalog paper. There are 1425 systems with a single candidate, 245 systems with two planet candidates, 84 systems with three planet candidates, 27 systems with four planet candidates, 8 systems with five planet candidates and one system with 6 planet candidates. Here we wish to investigate the overall distribution of planet sizes as a function of orbit; that is, do outer planets, in general, tend to be larger than inner planets?

A smaller planet (e.g., shallower transit) will be more easily detected if the period is short, simply from the fact that the number of observed transiting events increases with shorter orbital period. In a complementary manner, the larger planets are more easily detected at all periods, up to some period threshold where only $2-3$ transits are detected. Batalha et al. (2012) tabulate for each candidate the transit period, the transit duration, the impact parameter, and the signal-to-noise of the transit fits. The signal-to-noise ratios, coupled with the transit periods and the impact parameters, enables us to debias the sample for these observational detection efficiencies (see also Lissauer et al. 2011b).

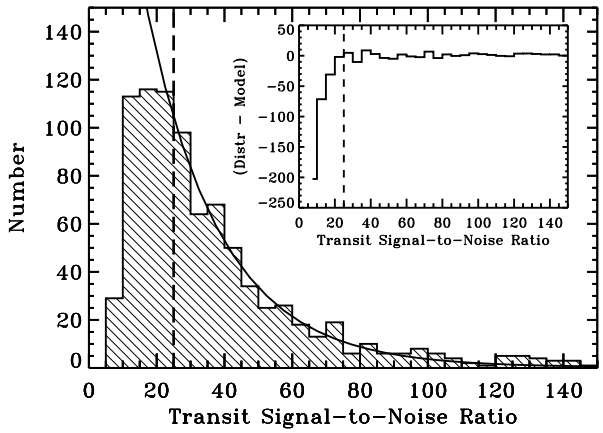

Figure 1. Distribution of the transit signal-to-noise ratio for all the detected "multiple" candidates from Batalha et al. (2012). The solid curve is an exponential fit to the SNR distribution, and the vertical dashed line at $SNR = 25$ marks approximately where the exponential no longer adequately describes the distribution (see inset figure).

The multiple candidate systems were identified primarily by searching the single candidate systems specifically for additional transiting planets. Thus, there could potentially be a detection bias of which we are unaware that is not found in the single candidate systems. However, no substantial difference between single planet systems and the multiple planet systems were found, except for the lack of hot Jupiters in the multiple planet systems (Latham et al. 2011; Steffen et al. 2012b). The overall size distribution of the planets and the signal-to-noise detection thresholds appear to be similar between the single candidate and multiple candidate systems.

To understand better the detection thresholds for the multiple candidate systems, we have used the distribution of the total transit signal-to-noise to estimate where the the distribution of planets in multiple systems appears to be complete (Figure 1). Assuming the signal-to-noise distribution can be characterized with an exponential function where the distribution is complete, we have used the point in the signal-to-noise distribution function where the exponential no longer adequately describes the distribution as the fiducial for completeness. Fitting the exponential, we find a turnover in detected samples at a $SNR \approx 25$. We use this SNR threshold to debias the radii-ratio distribution of planets in multiple-candidate systems.

The total signal-to-noise of all the detected transits for each planetary candidate is predicted for all the observed orbital periods within a system. A planet-pair is retained in the analysis only if the predicted total transit signal-

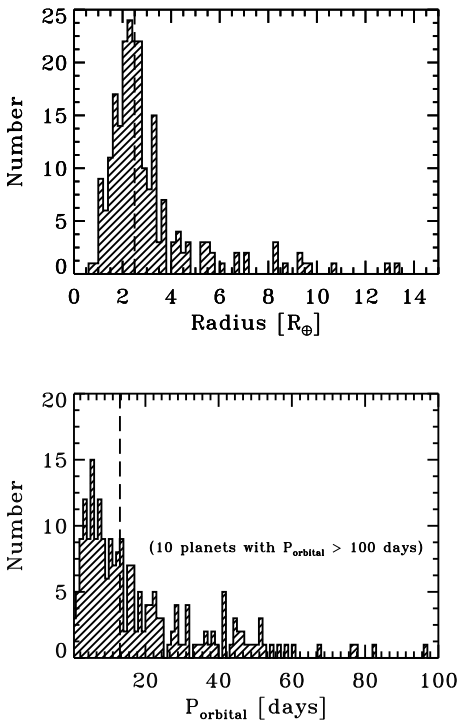

Figure 2. Distributions of the radii and orbital periods of the planets that are used in this study. The vertical dashed lines mark the median values of the distributions.

to-noise ratios for both planets at the orbital period of the other planet exceeds the signal-to-noise threshold of $SNR > 25$. The predicted signal-to-noise ratio is determined by scaling the measured total signal-to-noise ratio of the planet by the ratio of the orbital periods. Assuming all else is equal, the total signal-to-noise of all the detected transits for a given planet scales with the orbital period as $P^{-1/3}$.

For a given planet, the total signal-to-noise of all detected transits is proportional to the total number of points (n) detected in all of the transits (e.g., von Braun, Kane, & Ciardi 2009)

$$(S/N)_{transits} \propto (n)^{1/2} \propto (N \cdot n_t)^{1/2} \quad (1)$$

where N is the total number of individual transits detected, and n_t is the number of points detected within a single transit. The number of transits detected is inversely proportional to the orbital period ($N \propto 1/P$), and the number of points detected per transit is proportional to the transit duration ($n_t \propto t_{dur}$); thus, the total signal to noise of the detected transits can be parameterized as

$$(S/N)_{transits} \propto (t_{dur}/P)^{1/2} \quad (2)$$

The transit duration (t_{dur}) is proportional to the cube root of the orbital period ($t_{dur} \propto v_{orb}^{-1} \propto P^{1/3}$); thus, the total signal-to-noise ratio of the detected transits scales with the orbital period as

$$(S/N)_{transits} \propto (P^{1/3}/P)^{1/2} \propto P^{-1/3}. \quad (3)$$

An additional restriction on the sample was made such that no planet candidate was included that has an impact parameter of $b \geq 0.8$. At such high impact parameters, the transit parameters, particularly the transit depth (i.e., the planet radius), are less certain. Using the $SNR > 25$ detection threshold and the impact parameter restrictions, there are 96 multiple-candidate systems with 159 pairs of planets (228 individual planets) in the analysis.

All of the planet-pairs used in the analysis of this paper are summarized in Table 1; planets are labeled with roman numerals (I,II,III,IV,V,VI) in the order of increasing orbital period. These letters do not necessarily correspond to KOI fraction numbers (e.g., .01, .02, ...) nor do they correspond to the confirmed planet letters (e.g., *Kepler*-11b, *Kepler*-11c, ...). After the signal-to-noise and impact parameter cuts, the largest planet in the sample is $13R_\oplus$, and the median planet radius is $\approx 2.5R_\oplus$; the smallest planet retained in the sample has a radius of $0.75R_\oplus$. The orbital periods of the planets in this sample span 0.45 days to 331 days, with an median period of ~ 13.1 days. The distributions of the radii and orbit periods for the 228 planets retained in the sample are shown in Figure 2.

Previous work indicates that the detected planets in the *Kepler* multiple-candidate systems have mutual inclinations of $1^\circ - 3^\circ$ (Fabrycky et al. 2012b; Fang & Margot 2012). Due to the usual limitation of the transit technique in only detecting planets that are very nearly edge-on, the Kepler sample used here is naturally biased to systems of nearly coplanar planets. The prevalence of Kepler multiple-candidate systems shows that there is a large population of such systems with small planets and orbital periods of tens of days (Figure 2). It may be that other system architectures with higher mutual inclinations or different period ranges do not show the same trend in planet sizes that we describe herein.

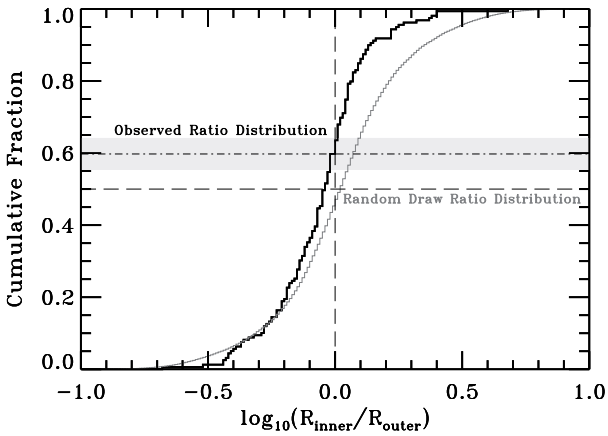

Figure 3. Observed cumulative distribution of the planet-radii ratios for all planet pairs (black histogram), and the predicted cumulative distribution for planet radii drawn randomly the measure planet sample (grey histogram). The horizontal dot-dash line marks the fraction of planet pairs with $R_{inner}/R_{outer} < 1$; the grey region marks the 1σ confidence interval for this fraction. The vertical dashed line marks the boundary where $R_{inner}/R_{outer} = 1$, and the horizontal dashed line marks the 50% fraction.

3. DISCUSSION

We have calculated the ratios of the inner planet radius to the outer planet radius for each unique pair of planets within a system (R_{inner}/R_{outer}), and the cumulative fraction distribution is displayed in Figure 3. If there were no preference for the ordering of planet sizes, the chance that a given planet-radii ratio is larger than unity would be equal to the chance that the ratio is below unity, and the cumulative fraction distribution would pass through 50% at $\log(R_{inner}/R_{outer}) = 0$ ($R_{inner}/R_{outer} = 1$).

In contrast, $59.7^{+4.1}_{-4.2}$% of the planet pairs are ordered such that the outer planet is larger than the inner planet ($R_{inner}/R_{outer} < 1$). The resulting fraction deviates from the null-hypothesis expectation value of 50% by $\approx 2.5\sigma$. The 1σ upper and lower confidence intervals are based upon the Clopper-Pearson binomial distribution confidence interval (Clopper & Pearson 1934). The Clopper-Pearson interval is a two-sided confidence interval and is based directly on the binomial distribution rather than an approximation to the binomial distribution. We do caution that in applying the Clopper-Pearson confidence interval there is an implicit assumption that all of elements of the sample are uncorrelated. Given that not all planet-pairs are from independent stellar systems, there may be a correlation between individual planet-pairs within a system (i.e., planet I is smaller than planet III because it is smaller than planet II), and the Clopper-Pearson confidence intervals may underestimate the true uncertainties in the fractions.

In addition to the confidence intervals, the significance of the observed fraction in comparison to the null hypothesis can be evaluated through the χ^2 statistic. The probability of the observed fraction ($96/159 = 59.7\%$) when compared to the expected fraction ($79.5/79.5 = 50\%$) yields $\chi^2 = 6.0$ with a probability of only 1.4% that the observed fraction is observed only by chance (see Table 2).

We also have performed three additional observational tests to assess if the observed fraction may be the result of an unrecognized bias in the sample. The first test repeated the above analysis, but for each unique planet pair, the measured radii were replaced with radii randomly drawn from the overall radius distribution as measured by Kepler; the same set of periods within a given system were retained. The same impact parameter and signal-to-noise restrictions described above (§2) were applied (e.g., if a planet radius was drawn that was too small to be detected at the orbital period ($SNR < 25$), a new radius was randomly drawn until the SNR threshold was met). The random draw was performed 10,000 times for each unique pair of planets, and the cumulative distribution of the planet-radii ratios for all of the random draws is displayed in Figure 3. As expected, the random draw distribution displays no size ordering preference; i.e., the fraction of planets with $R_{inner}/R_{outer} < 1$ is $\approx 50\%$. Based upon a Kolmogorov-Smirnov test, the observed distribution and the random draw distribution are not drawn from different parent distributions with only a probability of 3×10^{-8} – indicating that the observed planet radii ratio distribution has a preferential ordering such that smaller planets are in orbits interior to larger planets.

We also tested if the observed fraction of planet-radii ratios with $R_{inner}/R_{outer} < 1$ is dependent upon the signal-to-noise ratio threshold chosen. In Figure 4, the fraction of planet pairs where the inner planet is smaller than the outer planet is plotted as a function of the required signal-to-noise threshold. If no signal-to-noise threshold is required, the fraction is $> 70\%$, and as the signal-to-noise threshold is increased, the fraction systematically decreases and levels out near $\sim 60\%$. The higher fractions at a lower signal-to-noise threshold result from incompleteness of the sample (i.e., it is easier to detect larger planets at all orbital periods). As the signal-to-noise threshold is increased the fraction of planet-radii ratios below unity decreases, but does not systematically approach 50%, as would be expected if there was no preferential size ordering of the planets. Rather, the fraction asymptotically approaches 60% for $SNR_{threshold} > 20$, indicating the $SNR_{threshold} = 25$ threshold ensures that the analysis presented in Fig. 3 is based upon a sample not significantly biased by completeness.

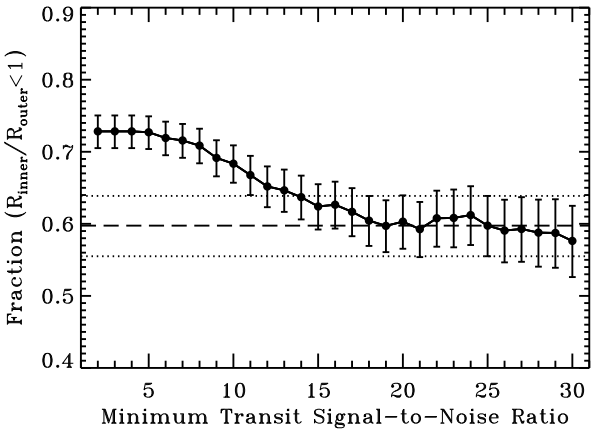

Figure 4. The observed fraction of planet pairs with $R_{inner}/R_{outer} < 1$ is plotted as a function of signal-to-noise cut-off, showing the fraction asymptotically approaches the a value of ~ 0.6 for $SNR \gtrsim 20$. The dashed line marks the observed fraction (and the 1σ confidence interval; dotted lines) for a $SNR_{threshold} = 25$ (from Fig. 3).

The final test performed was to determine if the observed fraction is dependent upon the maximum period of the outer planet (see Figure 5). Transit surveys are typically more complete at shorter orbit periods, and if there truly was no preference for planet size ordering, the fraction would decline and approach 50% as the maximum orbit period was decreased. Within the confidence intervals, the observed fractions are independent of the maximum outer orbital period and are consistent with the observed $\approx 60\%$ fraction for the entire sample. The fractions do not approach 50%, at shorter orbital period as would be expected for a random distribution. In fact, a slight (but not statistically significant) hint of a higher fraction is observed if the maximum period is $P < 20$ days.

Overall, if the ordering of planets within a given system was random such that there was no sequential ordering of the planets by size, the probabilities of a planet-radii ratio being above or below unity would be equal. But that is not what is observed; the three above tests (i.e., the random radius draw, the $SNR_{threshold}$, and the maximum outer orbital period), in combination with the χ^2

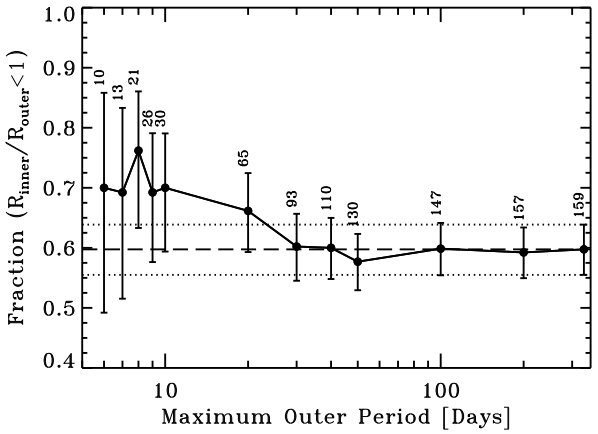

Figure 5. The observed fraction of planet pairs with $R_{inner}/R_{outer} < 1$ is plotted as a function of maximum outer orbital period cut-off, showing the fraction asymptotically approaches the value of ~ 0.6 for $P \gtrsim 20$. The dashed line marks the observed fraction for the whole sample; the dotted lines mark the 1σ confidence interval (from Fig. 3). The numbers above each data point indicate the number of planet-pairs that appear in that period bin ($P_{outer} < P_{max}$).

probability statistic and the confidence intervals, indicate that for $\approx 60\%$ (2.5σ) of the unique planet pairs within the Kepler multiple planet systems, the inner planet is smaller than the outer planet, with only a 1.4% chance of this being observed by chance. In the following subsections, we explore if and how the number of planets in the system, the orbital separation of the planets, the temperature of the stars, and the size of the planets themselves may affect the observed size hierarchy of the planets in multiple-planet systems.

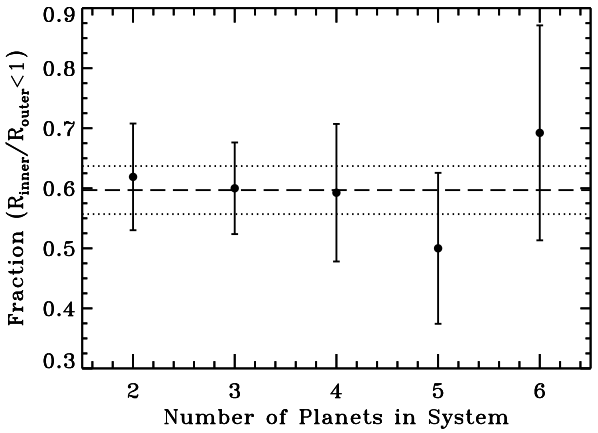

Figure 6. Observed fraction of planet-pairs with the inner planet being smaller the outer planet plotted as a function of the number of KOIs within a system.The dashed line marks the observed fraction for the whole sample; the dotted lines mark the 1σ confidence interval (from Fig. 3).

3.1. *The Number of Planets and Orbital Separation*

If formation and evolutionary mechanisms within a planetary system affect the size distribution and ordering of planets within a system, one might expect to observe differences in the size ordering as a function of the number of planets within a system. When the planets are divided into groups based upon the number of detected planetary candidates in the system (e.g., 2-, 3-, 4-, 5-, and 6-candidates), the fractions do not change appreciably from the fractions calculated for the entire sample set. This can be seen in the both χ^2 statistic (Table 2) where the χ^2 and associated probabilities are all comparable to each other and in Figure 6, where the observed fractions (with confidence intervals) are plotted and display no dependence on the number of planets in the system. While the number of systems with more than 3 planets have relatively large uncertainties and poor statistics because of the small numbers of the 4-, 5-, and 6-candidate systems, there is no correlation of the fraction of size-ordered planets with the number of planets within a planetary system.

It might be expected that planets nearer to the central star would undergo a higher level of photo-evaporation than planets at longer orbital periods and, thus, the relative sizes of the planets would be more extreme if the planets are more widely separated (larger orbital period ratio). To test this, we have plotted the planet-radii ratios vs. the orbital period ratios and the inner and outer planet orbital periods (Fig. 7). Using the Spearman nonparametric rank correlation function, we find that the distributions are likely uncorrelated. The correlation coefficients for the three distributions shown in Fig. 7 are 0.14, 0.22, and 0.10 with probabilities to be exceeded in the null hypothesis of 0.06, 0.004 and 0.08, respectively.

Additionally, to search for a non-zero slope that might indicate the planet-radii ratios are related to or dependent upon the period or period spacings, we have fitted a linear model[6] to each of the distributions. Each of the distributions are statistically consistent with a flat distribution as a function of period ratio and orbital period; the slopes of the fitted linear models were found to be 0.29 ± 0.15 for the radii ratios vs. period ratios (Fig. 7 top), 0.0009 ± 0.001 for the radii ratios vs. the inner orbital period (Fig. 7 middle), and -0.0002 ± 0.0005 for the radii ratios vs. the outer orbital period (Fig. 7 bottom). In general, we find no correlation between the orbital period separation (or orbital periods themselves) and the size-ordering of the planets.

3.2. *Stellar Temperature*

We have also explored whether there is a correlation between the distribution of planet-radii ratios and the effective temperature of the host stars. We have produced planet-radii ratio distributions, but separated out by the stellar temperature. We chose temperature ranges that roughly correspond to the spectral classification of M and K-stars (< 5000 K), G-stars ($5000 - 5800$ K), and F-stars (> 5800 K; Ciardi et al. 2011). The cumulative distributions of the planet-radii ratios for each of the stellar temperature groups are displayed in Figure 8.

Overall, all three distributions are shifted to lower ratios in comparison to the random draw distribution from Fig 3. Kolmogorov-Smirnov tests between the three distributions indicate that the three distributions do not result from different parent distributions with probabil-

[6] Fitting was done with an outlier resistant linear regression routine based upon Numerical Recipes (Press et al. 2007).

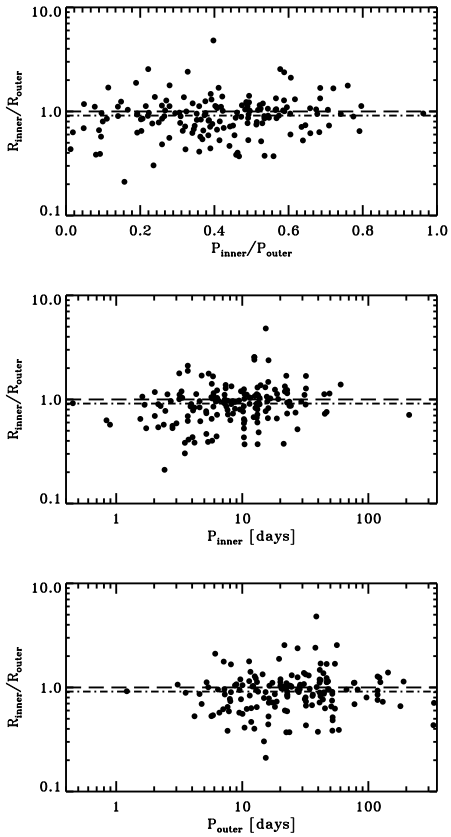

Figure 7. *Top:* Distribution of the planet-radii ratios as a function of the orbital period ratio. *Middle:* Distribution of the planet-radii ratio as a function of the inner planet orbital period. *Bottom:* Distribution of the planet-radii ratio as a function of the outer planet orbital period. In each panel, the horizontal dashed line marks unity, and the dot-dashed line delineates the median planet-radii ratio of 0.91 for the entire sample.

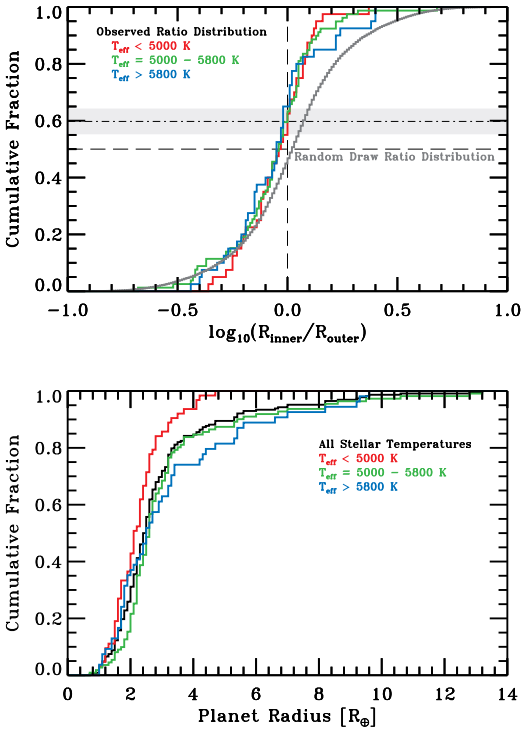

Figure 8. *Top:* Observed cumulative distributions of the planet-radii ratios as is displayed in Fig. 3, except the distributions have been separated out by stellar effective temperature and identified by the plot colors (as labeled in the plot). The plot markings as the same as those in Fig. 3. *Bottom:* Cumulative distributions of the individual radii for the planets that are used to determine the planet-radii ratios throughout the paper, separated out by stellar effective temperature (as labeled in the plot).

ities of $> 75\%$ - indicating that, in general, the preferential planet size ordering occurs at approximately the same level (i.e., $\approx 60\%$ the unique planet pairs have $R_{inner}/R_{outer} <$) across the stellar temperature range. A summary of the planet-radii ratios, the fraction of ratios that exhibit smaller inner planets, and the significance of those fractions based upon the confidence intervals and χ^2 statistic is given in Table 3 for each of the stellar temperature groups.

There does appear to be an slight trend such that as the stars become warmer they contain a larger fraction of planet-pairs sequentially ordered by radius. For the cooler stars (< 5000 K), this fraction is $55 \pm 9\%$, while for the warmer stars (> 5800 K), this fraction is $65 \pm 9\%$. The resulting χ^2 statistics for these three samples indicates that the observed fractions differ from the null hypothesis fraction of 50% more significantly for the warmer stars than for the cooler stars (Table 3). This trend could be a result of higher planetary evaporation rates associated with the higher luminosity stars or perhaps could result from the warmer (i.e., more massive) stars tending to contain larger (i.e., more massive) planets (see Figure 8 and Table 3).

The median planet radius does not vary significantly between the three stellar groups ($2.2 - 2.6 R_\oplus$; see Table 3), but the size of the largest planets in each group does. The G and F stars ($T_{eff} > 5000$ K) contain Saturn-sized and Jupiter-sized planets (in addition to smaller planets), while the cooler ($T_{eff} < 5000$ K) contain Neptune-sized planets and smaller (see Figure 8 and Table 3). In this sample, 15% of the planets around G-stars, and 25% of the planets around the F-stars, are Neptune-sized or larger; the cooler stars host only 6 (4%) planets larger than Neptune, and these four planets orbit three stars with effective temperatures of > 4900K (KOI 757, 884, 941). The absence of large planets around cooler stars is evident in the cumulative distribution of the planet radii (Fig. 8) and in the smaller median absolute deviations of the median planet radius for each stellar group (Table 3).

This paper is not intended to provide a discussion of the occurrence rates of planets or a detailed analysis of the size distribution of planets (e.g., Howard et al. 2012), but this may imply that the cooler (i.e., smaller) stars only produce smaller planets that do not preferentially follow a size hierarchy of planets . In fact, large planets around small stars may not form at all (Endl et al. 2003; Johnson et al. 2010) or, if they do, they may not survive their youth (e.g., van Eyken, Ciardi, von Braun et al. 2012). Thus, cool stars may only be left with a population of relatively small planets (Lopez et al. 2012). The warmer stars, in contrast, appear to host a larger array of planet sizes with a slightly higher preference for the larger planets (>Neptune-sized) to be in longer orbits exterior to the orbits of the smaller planets. Given

that there appears to be only a weak correlation with the planet-radii ratio and the orbital period (ratio), perhaps the formation and migration of large planets (perhaps in conjunction with photo-evaporation of the innermost planets) is necessary for a radius hierarchy to present.

3.3. *Planet Radius*

If hotter stars tend to show a planet radius hierarchy and the hotter stars also host relatively larger planets, then the planet hierarchy might be expected to be correlated with the planet size. In Figure 9, we compare the sizes of the planet radii for the inner and outer planets for each pair of planets within the sample. The overall planet-radii ratio is near unity but there is more scatter below than above the unity line (i.e., smaller planets are interior to larger planets). There are 36 planet-pairs where the outer planet is $> 50\%$ larger than the inner planet ($R_{inner}/R_{outer} \leq 0.67$); in contrast, there are only 13 planet-pairs where the inner planet is $> 50\%$ larger than the outer planet ($R_{inner}/R_{outer} \geq 1.5$).

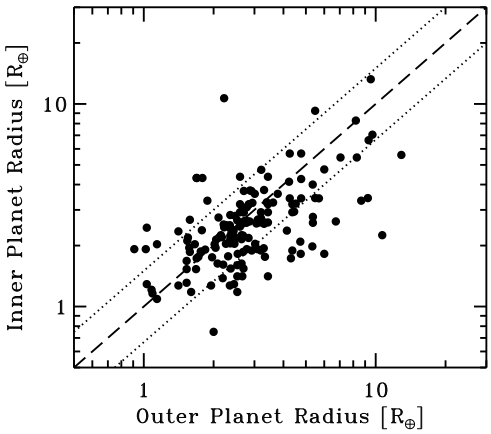

Figure 9. Comparison of the inner planet radius to the outer planet radius for each pair of planets, The dashed line delineates unity and the dotted lines mark the boundaries where one planet is 50% bigger than the planet to which it is compared (ratio = 0.67 if the outer planet is larger and ratio = 1.5 if the inner planet is larger).

For the planet-pairs that are in these relatively extreme ratio pairs, we have plotted the radii distributions of the candidates, separated out by inner and outer planet and by the sense of the ratio (see Figure 10). For the pairs where the outer planet is significantly larger, the ratio tends to be dominated by relatively large planets. Half (18/36) of the outer planets are Neptune-sized or larger ($> 4R_\oplus$), while only 25% (9/36) of the inner planets are very small (e.g., Earth-sized $< 1.5R_\oplus$) planets. In contrast, for those planet-pairs where the inner planet is much larger than the outer planet, the pairs are evenly split between relatively small outer planets (6/13 are $< 1.5R_\oplus$) and relatively large inner planets ($5/13 > 4R_\oplus$).

It appears that for there to be a planet radius hierarchy, one of the planets most often needs to be ∼Neptune-sized or larger. To explore this more closely, we have calculated the fraction of planet-pairs with ($R_{inner}/R_{outer} < 1$), if at least one planet is larger than some maximum planet radius (R_p), or if

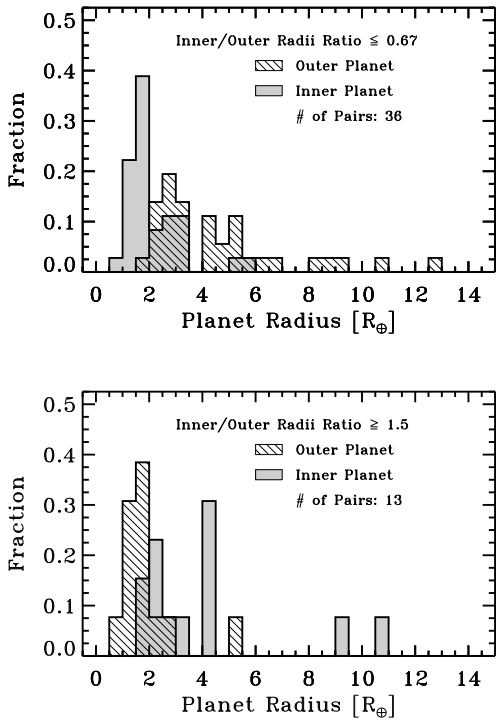

Figure 10. Distribution of the planet radii for those planet pairs where one planet is $> 50\%$ larger than the other planet. The top panel is for those planet pairs where the outer planet is larger than the inner planet ($R_{inner}/R_{outer} \leq 0.67$); the bottom panel is for those planet pairs where the inner planet is larger than the outer planet ($R_{inner}/R_{outer} \geq 1.5$);

both planets are smaller than that same maximum planet radius (R_p), or if both planets are larger than that same maximum planet radius. The fractions were calculated for maximum planet radii of $R_p = [1.5, 2.0, 2.5, 3.0, 3.5, 4.0, 4.5]R_\oplus$ (see Figure 11) and are tabulated in Table 4.

If planets-pairs with planets larger than $3R_\oplus$ are excluded, the fraction is very near 50% with little preference for sequential planet ordering, but if one planet in the pair is larger than $\sim 3R_\oplus$, the observed fraction of planet-pairs with ($R_{inner}/R_{outer} < 1$) is $68 \pm 6\%$ – a 3σ separation from the random ordering fraction of 50% (see Table 4). Based upon the χ^2 statistic and probability and the confidence intervals, the fraction of planet pairs is significantly above 50% only when Neptune-sized planets or larger are allowed in the pairs.

The fraction is most significant when Neptune-sized or larger planets are compared to planets of all sizes (top panel Fig 11); the χ^2 statistic are all > 4 with a $\lesssim 1\%$ probability that the non-50% fractions are achieved solely by chance. When the sizes of both planets are restricted to radii smaller than Neptune, the fractions remain near or below 50% (middle panel Fig 11 and Table 4), with a $\gtrsim 15\%$ probability of the observed fractions being generated by chance for the null-hypothesis distribution. When both planets within a planet pair are restricted to planets larger than a certain radius, sequential ordering of the planet sizes is still apparent, but is less significant (bottom panel Fig 11 and Table 4). If both planets in a pair are $\gtrsim 3.0R_\oplus$, then the observed fraction of planet-pairs where the inner planet is smaller than the

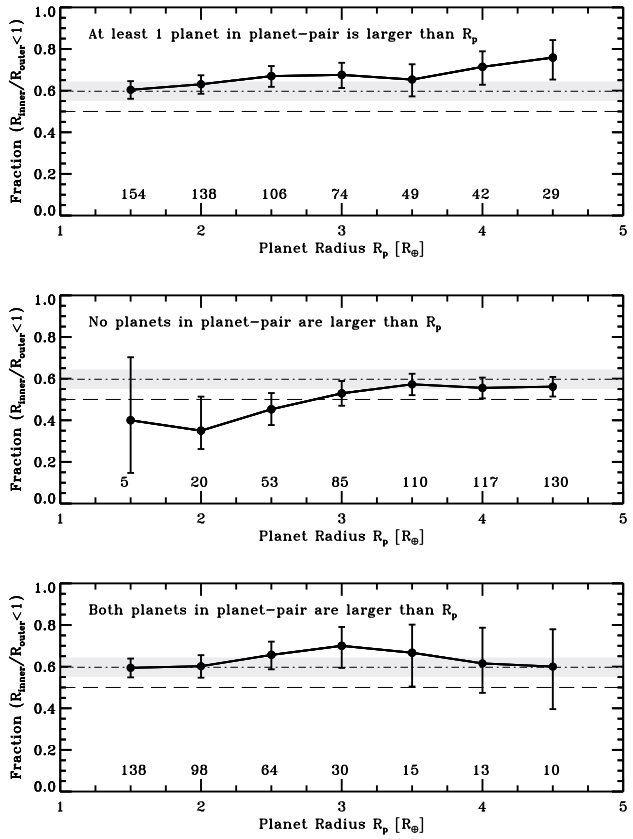

Figure 11. The fraction of planet-pairs with ($R_{inner}/R_{outer} < 1$) are plotted as a function of maximum planet radius. In the top panel, only those planet-pairs are included that have at least one planet that is larger than a planet radius R_p. In the middle panel, only those planet-pairs are included where both planets are smaller than a planet radius R_p. In the bottom panel, only those planet-pairs are included where both planets are larger than a planet radius R_p. The numbers underneath each data point list the number of pairs in that bin. In each panel, the dashed-dot line and grey area delineate the fraction and uncertainties found for the entire sample (from Fig. 3); the dashed line delineates the 50% fraction.

outer planet are consistent with no planet size hierarchy. These results suggest that the size ordering primarily occurs when a system contains both superearth-sized (or earth-sized) planets *and* Neptune-sized or larger planets, and may be a direct result shepherding of smaller inner planets by larger outer planets (Raymond et al. 2008).

4. SUMMARY

We have performed a study of the relative sizes of planets within the multiple candidate systems using the *Kepler* planetary candidate list (Batalha et al. 2012). For each multiple planet system, we have compared the radius of each planet to the radius of every other planet within a planetary system, after correcting for detection biases. We find that for planet-pairs for which one or both objects is approximately Neptune-sized for larger, the larger planet is most often the planet with the longer period, while no such size–location correlation is seen for pairs of planets when both planets are smaller than Neptune. Overall, for all planets-pairs in the sample, $60 \pm 4\%$ of the unique planet pairs are structured in a hierarchical manner such that the inner planet is smaller than the outer planet. If at least one planet in the planet-pair is Neptune-sized or larger ($\gtrsim 3R_\oplus$), the fraction of inner planets being smaller than outer planets is $\approx 68 \pm 6\%$. However, if both planets are smaller than Neptune, then the fraction is consistent with random planet ordering ($53 \pm 6\%$) with no apparent size hierarchy.

The planet radius size hierarchy may be a natural consequence of planetary formation and evolution. In particular, the sequential ordering may be a result of a combination of core accretion, migration, and evolution. Core accretion models predict that smaller planets are expected to form prior to and interior to the giant planets (Zhou et al. 2005). Additionally, larger planets formed further out may migrate inwards, shepherding smaller planets inward as the planets move (Raymond et al. 2008).

This scenario is consistent with the planet size hierarchy being observed for planets pairs involving Neptune-sized planets, but being absent for small planet pairs and for the planets around cool stars. For the cooler stars, the forming planets may begin migrating prior to starting rapid gas accretion (e.g., Ida & Lin 2005), coupled with a lower extreme ultraviolet luminosity that is not capable of substantially evaporating the planets (Lopez et al. 2012). For example, Lopez et al. (2012) suggest that the *Kepler*-11 planets did not form *in situ*, but rather, the planets formed beyond the snow line, migrated inwards, and were evaporated by the star to their present sizes.

These scenarios (perhaps, all in concert) predict a radius hierarchy of planets as a function of orbital distance from the central host star, in particular, predicting that Neptune-sized and larger planets are outside super-Earth and terrestrial-sized planets. As *Kepler* discovers more planets in longer orbital periods, it will be interesting to learn if our Solar System is indeed typical of the planetary architectures found in the Galaxy.

Kepler was competitively selected as the 10th NASA Discovery mission. The authors thank the many people who have made *Kepler* such a success. This paper includes data collected by the *Kepler* mission; funding for the *Kepler* mission is provided by the NASA Science Mission directorate.This research has made use of the NASA Exoplanet Archive, which is operated by the California Institute of Technology, under contract with the National Aeronautics and Space Administration under the Exoplanet Exploration Program. D.C.F. acknowledges NASA support through Hubble Fellowship grant HF-51272.01-A, awarded by STScI, operated by AURA under contract NAS 5-26555. DRC would like to thank the referee, the *Kepler* team, Bill Borucki, Geoff Marcy, Stephen Kane, Peter Plavchan, Kaspar von Braun, Teresa Ciardi, and Jim Grubbs for very insightful and inspirational comments and discussions in the formation of this paper.

REFERENCES

Batalha, N. M. et al. 2011, ApJ, 729, 27
Batalha, N. M., Rowe, J. F., Bryson, S. T., et al. 2012, arXiv:1202.5852
Borucki, W. J., et al. 2010, Science, 327, 977
Borucki, W. J., Koch, D. G., Basri, G., et al. 2011, ApJ, 736, 19
Ciardi, D. R. et al., 2011, AJ, 141, 108
Clopper, C.J., & Pearson, E.S., 1934, Biometrika, 26, 404

Endl, M., Cochran, W. D., Tull, R. G., & MacQueen, P. J. 2003, AJ, 126, 3099
Fabrycky, D. C., Ford, E. B., Steffen, J. H., et al. 2012, ApJ, 750, 114
Fabrycky, D. C.et al. 2012, ApJ, submitted, arXiv:1202.6328v2
Fang, J., & Margot, J.-L. 2012, arXiv:1207.5250
Fressin, F., Torres, G., Rowe, J. F., et al. 2012, Nature, 482, 195
Gautier, T. N., III, Charbonneau, D., Rowe, J. F., et al. 2012, ApJ, 749, 15
Howard, A. W., Marcy, G. W., Bryson, S. T., et al. 2012, ApJS, 201, 15
Ida, S. & Lin, D. N. C. 2005, ApJ, 626, 1045
Johnson, J. A., Aller, K. M., Howard, A. W., & Crepp, J. R. 2010, PASP, 122, 905
Latham, D. W., et al. 2011. ApJ, 732, L24
Lissauer, J. J., Fabrycky, D. C., Ford, E. B., et al. 2011, Nature, 470, 53
Lissauer, J. J., Ragozzine, D., Fabrycky, D. C., et al. 2011, ApJS, 197, 8
Lissauer, J. J., Marcy, G. W., Rowe, J. F., et al. 2012, ApJ, 750, 112
Lopez, E. D., Fortney, J. J., & Miller, N. K. 2012, arXiv:1205.0010
Migaszewski, C., Slonina, M., & Gozdziewski, K. 2012, arXiv:1205.0822
Morton, T. D., & Johnson, J. A. 2011, ApJ, 738, 170
Muirhead, P. S., Hamren, K., Schlawin, E., et al. 2012, ApJ, 750, L37
Orosz, J. A., Welsh, W. F., Carter, J. A., et al. 2012, Science, 337, 1511
Press, William H.; Teukolsky, Saul A.; Vetterling, William T.; Flannery, Brian P. 2007, Numerical Recipes: The Art of Scientific Computing (3rd ed.). New York: Cambridge University Press
Raymond, S. N., Barnes, R., & Mandell, A. M. 2008, MNRAS, 384, 663
Raymond, S. N., Armitage, P. J., Moro-Martín, A., et al. 2012, A&A, 541, A11
Santerne, A., Díaz, R. F., Moutou, C., et al. 2012, arXiv:1206.0601
Steffen, J. H., Fabrycky, D. C., Ford, E. B., et al. 2012, MNRAS, 421, 2342
Steffen, J. H., Ragozzine, D., Fabrycky, D. C., et al. 2012, Proceedings of the National Academy of Science, 109, 7982 (arXiv:1205.2309)
Torres, G. et al. 2011 ApJ, 727, 24
Wright, J. T., Upadhyay, S., Marcy, G. W., et al. 2009, ApJ, 693, 1084
van Eyken, J. C., Ciardi, D. R., von Braun, K., et al. 2012, ApJ, 755, 42
von Braun, K., Kane, S. R., & Ciardi, D. R. 2009, ApJ, 702, 779
Walsh, K. J., Morbidelli, A., Raymond, S. N., O'Brien, D. P., & Mandell, A. M. 2011, Nature, 475, 206
Zhou, J.-L., Aarseth, S. J., Lin, D. N. C., & Nagasawa, M. 2005, ApJ, 631, L85

Table 1
Summary of Planet-Radii Ratios

KOI	Stellar Temp (K)	Planet Pair	Inner Planet Radius ($R_\oplus$)	Inner Planet Period (days)	Inner Planet Transit SNR	Inner Planet Impact Par.	Outer Planet Radius ($R_\oplus$)	Outer Planet Period (days)	Outer Planet Transit SNR	Outer Planet Impact Par.	Planet Radii Ratio R_{inner}/R_{outer}
KOIs with 2 Candidates											
K00072	5627	I/II	1.38	0.837	139	0.17	2.19	45.294	122	0.11	0.630
K00108	5975	I/II	2.94	15.965	84	0.79	4.45	179.600	111	0.62	0.661
K00119	5380	I/II	3.76	49.184	152	0.55	3.30	190.310	63	0.69	1.139
K00123	5871	I/II	2.64	6.482	98	0.56	2.71	21.222	78	0.01	0.974
K00150	5538	I/II	2.63	8.409	106	0.73	2.73	28.574	81	0.76	0.963
K00209	6221	I/II	5.44	18.795	217	0.51	8.29	50.790	287	0.40	0.656
K00222	4353	I/II	2.03	6.312	85	0.71	1.66	12.794	43	0.72	1.223
K00223	5128	I/II	2.52	3.177	90	0.78	2.27	41.008	32	0.69	1.110
K00271	6169	I/II	2.48	29.392	72	0.71	2.60	48.630	54	0.79	0.954
K00275	5795	I/II	1.95	15.791	55	0.03	2.04	82.199	27	0.60	0.956
K00312	6158	I/II	1.91	11.578	41	0.70	1.84	16.399	40	0.58	1.038
K00313	5348	I/II	1.61	8.436	54	0.32	2.20	18.735	55	0.73	0.732
K00386	5969	I/II	3.25	31.158	57	0.02	2.94	76.732	28	0.55	1.105
K00413	5236	I/II	2.75	15.228	52	0.67	2.10	24.674	26	0.65	1.310
K00431	5249	I/II	2.80	18.870	60	0.60	2.48	46.901	34	0.68	1.129
K00433	5237	I/II	5.60	4.030	127	0.65	12.90	328.240	158	0.77	0.434
K00446	4492	I/II	1.76	16.709	33	0.62	1.72	28.551	34	0.05	1.023
K00448	4264	I/II	1.77	10.139	56	0.74	2.31	43.608	66	0.66	0.766
K00464	5362	I/II	2.63	5.350	75	0.58	6.73	58.362	263	0.20	0.391
K00475	5056	I/II	2.04	8.181	37	0.58	2.26	15.313	34	0.68	0.903
K00509	5437	I/II	2.24	4.167	45	0.09	2.68	11.463	32	0.74	0.836
K00518	4565	I/II	2.11	13.981	68	0.71	1.54	44.000	33	0.49	1.370
K00638	5722	I/II	3.60	23.636	53	0.02	3.78	67.093	39	0.27	0.952
K00657	4632	I/II	1.63	4.069	43	0.63	2.08	16.282	46	0.74	0.784
K00672	5524	I/II	2.60	16.087	43	0.71	3.15	41.749	70	0.11	0.825
K00676	4367	I/II	2.56	2.453	255	0.70	3.30	7.972	348	0.57	0.776
K00693	6121	I/II	1.87	15.660	48	0.50	1.76	28.779	23	0.64	1.062
K00708	6036	I/II	1.82	7.693	43	0.74	2.54	17.406	68	0.70	0.717
K00800	5938	I/II	3.27	2.711	48	0.76	3.39	7.212	36	0.77	0.965
K00841	5399	I/II	5.44	15.334	83	0.74	7.05	31.331	117	0.74	0.772
K00842	4497	I/II	2.04	12.718	43	0.31	2.46	36.065	44	0.42	0.829
K00853	4842	I/II	2.38	8.204	48	0.12	1.78	14.496	22	0.02	1.337
K00870	4590	I/II	2.52	5.912	56	0.76	2.35	8.986	47	0.73	1.072
K00877	4500	I/II	2.42	5.955	54	0.73	2.37	12.039	36	0.79	1.021
K00896	5190	I/II	3.22	6.308	68	0.52	4.52	16.239	91	0.57	0.712
K00936	3684	I/II	1.54	0.893	72	0.75	2.69	9.468	96	0.76	0.572
K00951	4767	I/II	3.74	13.197	101	0.39	2.87	33.653	36	0.58	1.303
K00988	5218	I/II	2.20	10.381	67	0.02	2.17	24.570	37	0.67	1.014
K01236	6562	I/II	2.04	12.309	40	0.01	3.02	35.743	64	0.37	0.675
K01270	5145	I/II	2.19	5.729	45	0.58	1.55	11.609	22	0.01	1.413
K01781	4977	I/II	1.94	3.005	81	0.19	3.29	7.834	172	0.01	0.590

Table 1 — *Continued*

KOI	Stellar Temp (K)	Planet Pair	Inner Planet Radius ($R_\oplus$)	Inner Planet Period (days)	Inner Planet Transit SNR	Inner Planet Impact Par.	Outer Planet Radius ($R_\oplus$)	Outer Planet Period (days)	Outer Planet Transit SNR	Outer Planet Impact Par.	Planet Radii Ratio R_{inner}/R_{outer}
K01824	5978	I/II	1.75	1.678	53	0.70	1.97	3.554	50	0.69	0.888
KOIs with 3 Candidates											
K00085	6172	I/II	1.27	2.155	72	0.71	2.35	5.860	154	0.77	0.540
K00085	6172	I/III	1.27	2.155	72	0.71	1.41	8.131	53	0.78	0.901
K00085	6172	II/III	2.35	5.860	154	0.77	1.41	8.131	53	0.78	1.667
K00111	5711	I/II	2.14	11.427	96	0.53	2.05	23.668	71	0.55	1.044
K00111	5711	I/III	2.14	11.427	96	0.53	2.36	51.756	75	0.57	0.907
K00111	5711	II/III	2.05	23.668	71	0.55	2.36	51.756	75	0.57	0.869
K00115	6202	II/III	3.33	5.412	144	0.43	1.88	7.126	41	0.55	1.771
K00137	5385	I/II	1.82	3.505	44	0.71	4.75	7.641	299	0.50	0.383
K00137	5385	I/III	1.82	3.505	44	0.71	6.00	14.858	305	0.72	0.303
K00137	5385	II/III	4.75	7.641	299	0.50	6.00	14.858	305	0.72	0.792
K00152	6187	I/II	2.59	13.484	58	0.34	2.77	27.402	57	0.07	0.935
K00152	6187	I/III	2.59	13.484	58	0.34	5.36	52.091	158	0.00	0.483
K00152	6187	II/III	2.77	27.402	57	0.07	5.36	52.091	158	0.00	0.517
K00156	4619	I/II	1.18	5.188	38	0.53	1.60	8.041	54	0.64	0.738
K00156	4619	I/III	1.18	5.188	38	0.53	2.53	11.776	131	0.69	0.466
K00156	4619	II/III	1.60	8.041	54	0.64	2.53	11.776	131	0.69	0.632
K00284	5925	I/II	1.09	6.178	32	0.38	1.14	6.415	35	0.19	0.956
K00343	5744	I/II	1.86	2.024	72	0.63	2.68	4.762	108	0.63	0.694
K00343	5744	I/III	1.86	2.024	72	0.63	1.58	41.809	20	0.53	1.177
K00343	5744	II/III	2.68	4.762	108	0.63	1.58	41.809	20	0.53	1.696
K00351	6103	II/III	6.62	210.590	144	0.22	9.32	331.640	211	0.19	0.710
K00377	5777	II/III	8.28	19.273	136	0.35	8.21	38.907	81	0.62	1.009
K00398	5101	I/II	1.76	1.729	37	0.24	3.33	4.180	102	0.00	0.529
K00398	5101	II/III	3.33	4.180	102	0.00	8.66	51.846	215	0.66	0.385
K00408	5631	I/II	3.72	7.382	96	0.79	2.91	12.560	52	0.77	1.278
K00408	5631	I/III	3.72	7.382	96	0.79	2.70	30.827	34	0.79	1.378
K00408	5631	II/III	2.91	12.560	52	0.77	2.70	30.827	34	0.79	1.078
K00481	5227	I/II	1.54	1.554	43	0.71	2.37	7.650	56	0.76	0.650
K00481	5227	II/III	2.37	7.650	56	0.76	2.44	34.260	39	0.73	0.971
K00528	5448	I/III	2.62	9.577	55	0.48	3.27	96.671	32	0.71	0.801
K00620	5803	I/III	7.05	45.155	132	0.03	9.68	130.180	279	0.06	0.728
K00658	5676	I/II	2.03	3.163	68	0.53	2.02	5.371	52	0.65	1.005
K00658	5676	I/III	2.03	3.163	68	0.53	1.14	11.329	17	0.01	1.781
K00665	5864	I/II	1.16	1.612	34	0.69	1.09	3.072	27	0.64	1.064
K00701	4807	I/II	1.27	5.715	55	0.46	1.95	18.164	71	0.66	0.651
K00701	4807	II/III	1.95	18.164	71	0.66	1.57	122.390	34	0.29	1.242
K00711	5502	II/III	3.18	44.699	51	0.61	2.83	124.520	35	0.49	1.124
K00718	5788	I/II	2.57	4.585	67	0.34	3.06	22.714	58	0.29	0.840
K00718	5788	I/III	2.57	4.585	67	0.34	2.67	47.904	27	0.68	0.963
K00718	5788	II/III	3.06	22.714	58	0.29	2.67	47.904	27	0.68	1.146
K00723	5244	I/III	3.26	3.937	72	0.79	3.61	28.082	60	0.58	0.903
K00757	4956	I/II	2.09	6.253	34	0.00	4.73	16.068	120	0.25	0.442
K00757	4956	II/III	4.73	16.068	120	0.25	3.21	41.192	40	0.35	1.474
K00806	5461	II/III	13.24	60.322	366	0.37	9.52	143.210	69	0.34	1.391
K00864	5337	I/III	2.51	4.312	63	0.14	2.23	20.050	30	0.00	1.126
K00884	4931	II/III	4.13	9.439	143	0.48	4.23	20.476	73	0.70	0.976
K00898	4648	I/II	2.18	5.170	35	0.64	2.83	9.771	47	0.68	0.770
K00898	4648	II/III	2.83	9.771	47	0.68	2.36	20.089	28	0.59	1.199
K00921	5046	II/III	2.66	10.281	43	0.69	3.09	18.119	46	0.70	0.861
K00941	4998	I/II	2.37	2.383	38	0.53	4.14	6.582	99	0.03	0.572
K00961	4188	I/II	2.63	0.453	100	0.69	2.86	1.214	73	0.77	0.920
K01576	5445	I/II	3.20	10.415	64	0.68	2.84	13.084	50	0.65	1.127
K01835	5004	I/II	2.69	2.248	43	0.44	3.11	4.580	37	0.67	0.865
K01860	5708	II/III	2.44	6.319	46	0.46	2.36	12.209	36	0.35	1.034
K01867	3892	I/II	1.21	2.549	37	0.40	1.08	5.212	25	0.31	1.120
KOIs with 4 Candidates											
K00094	6217	I/II	1.41	3.743	35	0.16	3.43	10.423	78	0.01	0.411
K00094	6217	II/III	3.43	10.423	78	0.01	9.25	22.343	455	0.30	0.371
K00094	6217	II/IV	3.43	10.423	78	0.01	5.48	54.319	206	0.38	0.626
K00094	6217	III/IV	9.25	22.343	455	0.30	5.48	54.319	206	0.38	1.688
K00191	5495	II/III	2.25	2.418	53	0.55	10.67	15.358	642	0.59	0.211
K00191	5495	III/IV	10.67	15.358	642	0.59	2.22	38.651	21	0.52	4.806
K00245	5288	II/III	0.75	21.301	49	0.76	2.00	39.792	282	0.79	0.375
K00571	3881	I/II	1.31	3.887	36	0.76	1.53	7.267	36	0.76	0.856
K00571	3881	II/III	1.53	7.267	36	0.76	1.68	13.343	36	0.79	0.911
K00571	3881	II/IV	1.53	7.267	36	0.76	1.53	22.407	27	0.78	1.000
K00571	3881	III/IV	1.68	13.343	36	0.79	1.53	22.407	27	0.78	1.098
K00720	5123	I/II	1.41	2.796	58	0.08	2.66	5.690	124	0.40	0.530
K00720	5123	I/III	1.41	2.796	58	0.08	2.53	10.041	87	0.64	0.557
K00720	5123	II/III	2.66	5.690	124	0.40	2.53	10.041	87	0.64	1.051
K00733	5038	II/III	2.54	5.925	60	0.14	2.21	11.349	35	0.31	1.149

Table 1 — *Continued*

KOI	Stellar Temp (K)	Planet Pair	Inner Planet Radius ($R_\oplus$)	Inner Planet Period (days)	Inner Planet Transit SNR	Inner Planet Impact Par.	Outer Planet Radius ($R_\oplus$)	Outer Planet Period (days)	Outer Planet Transit SNR	Outer Planet Impact Par.	Planet Radii Ratio R_{inner}/R_{outer}
K00812	4097	I/III	2.19	3.340	54	0.13	2.11	20.060	28	0.35	1.038
K00834	5614	III/IV	1.98	13.233	33	0.38	5.33	23.653	154	0.38	0.371
K00869	5085	II/IV	2.73	7.490	43	0.47	3.20	36.280	34	0.42	0.853
K00880	5512	III/IV	4.00	26.442	48	0.64	5.35	51.530	109	0.02	0.748
K00952	3911	II/III	2.25	5.901	47	0.72	2.15	8.752	35	0.77	1.047
K00952	3911	II/IV	2.25	5.901	47	0.72	2.64	22.780	38	0.77	0.852
K00952	3911	III/IV	2.15	8.752	35	0.77	2.64	22.780	38	0.77	0.814
K01557	4783	II/IV	3.60	3.296	122	0.52	3.01	9.653	70	0.30	1.196
K01567	5027	II/III	2.46	7.240	34	0.36	2.22	17.326	23	0.00	1.108
K01930	5897	II/III	2.21	13.726	38	0.60	2.14	24.310	31	0.62	1.033
K01930	5897	II/IV	2.21	13.726	38	0.60	2.46	44.431	29	0.66	0.898
K01930	5897	III/IV	2.14	24.310	31	0.62	2.46	44.431	29	0.66	0.870
KOIs with 5 Candidates											
K00070	5443	I/II	1.92	3.696	134	0.60	0.91	6.098	23	0.66	2.110
K00070	5443	I/III	1.92	3.696	134	0.60	3.09	10.854	260	0.55	0.621
K00070	5443	I/IV	1.92	3.696	134	0.60	1.02	19.577	18	0.74	1.882
K00070	5443	I/V	1.92	3.696	134	0.60	2.78	77.611	103	0.55	0.691
K00070	5443	III/V	3.09	10.854	260	0.55	2.78	77.611	103	0.55	1.112
K00082	4908	III/IV	1.29	10.311	79	0.71	2.45	16.145	172	0.73	0.527
K00082	4908	III/V	1.29	10.311	79	0.71	1.03	27.453	28	0.79	1.252
K00082	4908	IV/V	2.45	16.145	172	0.73	1.03	27.453	28	0.79	2.379
K00232	5868	I/II	1.73	5.766	41	0.40	4.31	12.465	207	0.43	0.401
K00232	5868	I/III	1.73	5.766	41	0.40	1.69	21.587	21	0.67	1.024
K00232	5868	II/III	4.31	12.465	207	0.43	1.69	21.587	21	0.67	2.550
K00232	5868	II/IV	4.31	12.465	207	0.43	1.79	37.996	21	0.56	2.408
K00232	5868	II/V	4.31	12.465	207	0.43	1.69	56.255	19	0.38	2.550
K00500	4613	III/IV	1.63	4.645	30	0.72	2.64	7.053	59	0.71	0.617
K00500	4613	IV/V	2.64	7.053	59	0.71	2.79	9.522	55	0.79	0.946
K00707	5904	II/III	3.42	13.175	37	0.77	5.69	21.775	80	0.77	0.601
K00707	5904	II/IV	3.42	13.175	37	0.77	4.26	31.784	42	0.77	0.803
K00707	5904	II/V	3.42	13.175	37	0.77	4.77	41.029	51	0.77	0.717
K00707	5904	III/IV	5.69	21.775	80	0.77	4.26	31.784	42	0.77	1.336
K00707	5904	III/V	5.69	21.775	80	0.77	4.77	41.029	51	0.77	1.193
K00707	5904	IV/V	4.26	31.784	42	0.77	4.77	41.029	51	0.77	0.893
K01589	5755	II/III	2.23	8.726	30	0.72	2.36	12.882	27	0.79	0.945
KOIs with 6 Candidates											
K00157	5685	I/II	1.89	10.304	38	0.34	2.92	13.024	67	0.35	0.647
K00157	5685	I/III	1.89	10.304	38	0.34	3.20	22.686	73	0.33	0.591
K00157	5685	I/IV	1.89	10.304	38	0.34	4.37	31.995	87	0.79	0.432
K00157	5685	II/III	2.92	13.024	67	0.35	3.20	22.686	73	0.33	0.913
K00157	5685	II/IV	2.92	13.024	67	0.35	4.37	31.995	87	0.79	0.668
K00157	5685	II/V	2.92	13.024	67	0.35	2.60	46.687	40	0.49	1.123
K00157	5685	II/VI	2.92	13.024	67	0.35	3.43	118.360	54	0.36	0.851
K00157	5685	III/IV	3.20	22.686	73	0.33	4.37	31.995	87	0.79	0.732
K00157	5685	III/V	3.20	22.686	73	0.33	2.60	46.687	40	0.49	1.231
K00157	5685	III/VI	3.20	22.686	73	0.33	3.43	118.360	54	0.36	0.933
K00157	5685	IV/V	4.37	31.995	87	0.79	2.60	46.687	40	0.49	1.681
K00157	5685	IV/VI	4.37	31.995	87	0.79	3.43	118.360	54	0.36	1.274
K00157	5685	V/VI	2.60	46.687	40	0.49	3.43	118.360	54	0.36	0.758

Table 2
Planet-Radii Ratios Summary Grouped by Number of KOIs

	All Systems	2-KOI Systems	3-KOI Systems	4-KOI Systems	5-KOI Systems	6-KOI Systems
# of Stellar Systems	96	42	33	14	6	1
# of R_{inner}/R_{outer} Pairs	159	42	55	27	22	13
Number $R_{inner}/R_{outer} < 1$	95	26	33	16	11	9
Number $R_{inner}/R_{outer} > 1$	64	16	22	11	11	4
χ^2 Statistic[a]	6.0	2.4	2.2	0.93	0.0	1.9
χ^2 Probability[a]	0.014	0.13	0.14	0.34	1.0	0.16
Fraction $R_{inner}/R_{outer} < 1$	0.597	0.619	0.600	0.592	0.500	0.692
Lower 1σ Confidence	0.042	0.089	0.076	0.115	0.126	0.179
Upper 1σ Confidence	0.041	0.082	0.072	0.107	0.126	0.140

[a] The χ^2 statistic and probability is based upon comparison of the observed fractions to the null hypothesis fractions of 50%.

Table 3
Planet-Radii Ratios Grouped by Stellar Temperature

	> 5800 K Stars	$5000 - 5800$ K Stars	< 5000K Stars
# of Stellar Systems	22	47	27
# of R_{inner}/R_{outer} Pairs	40	79	40
Number $R_{inner}/R_{outer} < 1$	26	47	22
Number $R_{inner}/R_{outer} > 1$	14	32	18
χ^2 Statistic	3.6	2.9	0.4
χ^2 Probability	0.06	0.09	0.50
Fraction $R_{inner}/R_{outer} < 1$	0.650	0.594	0.550
Lower 1σ Confidence	0.091	0.062	0.091
Upper 1σ Confidence	0.082	0.060	0.088
Median Planet Radius $[R_\oplus]$	2.59	2.63	2.19
Med. Abs. Dev. $[R_\oplus]$	1.49	1.18	0.61
Min. Planet Radius $[R_\oplus]$	1.09	0.75	1.03
Max. Planet Radius $[R_\oplus]$	9.68	13.2	4.73

Table 4
Planet-Radii Ratios Summary Group by Maximum Planet Radius

$R_p =$	$1.5R_\oplus$	$2.0R_\oplus$	$2.5R_\oplus$	$3.0R_\oplus$	$3.5R_\oplus$	$4.0R_\oplus$	$4.5R_\oplus$
At least one planet in planet-pair is larger than R_p							
# of Stellar Systems	93	86	63	44	29	23	18
# of R_{inner}/R_{outer} Pairs	154	138	106	74	49	42	29
Number $R_{inner}/R_{outer} < 1$	93	87	71	50	32	30	22
Number $R_{inner}/R_{outer} > 1$	61	51	35	24	17	12	7
χ^2 Statistic	6.7	9.4	12.2	9.1	4.6	7.7	7.8
χ^2 Probability	0.009	0.002	0.0005	0.003	0.03	0.005	0.005
Fraction $R_{inner}/R_{outer} < 1$	0.603	0.630	0.670	0.676	0.653	0.714	0.759
Lower 1σ Confidence	0.043	0.045	0.052	0.063	0.081	0.086	0.105
Upper 1σ Confidence	0.041	0.043	0.048	0.058	0.073	0.075	0.084
No planets in planet-pair are larger than R_p							
# of Stellar Systems	5	15	38	58	73	78	82
# of R_{inner}/R_{outer} Pairs	5	20	53	85	110	117	130
Number $R_{inner}/R_{outer} < 1$	2	7	24	45	63	65	73
Number $R_{inner}/R_{outer} > 1$	3	13	29	40	47	52	57
χ^2 Statistic	0.0	1.8	0.47	0.29	2.3	1.4	1.9
χ^2 Probability	1.0	0.18	0.49	0.59	0.13	0.23	0.16
Fraction $R_{inner}/R_{outer} < 1$	0.400	0.350	0.453	0.529	0.572	0.555	0.561
Lower 1σ Confidence	0.253	0.088	0.076	0.060	0.052	0.050	0.048
Upper 1σ Confidence	0.302	0.164	0.078	0.059	0.051	0.049	0.046
Both planets in planet-pair are larger than R_p							
# of Stellar Systems	89	67	42	21	13	11	10
# of R_{inner}/R_{outer} Pairs	138	98	64	30	15	13	10
Number $R_{inner}/R_{outer} < 1$	82	59	42	21	10	8	6
Number $R_{inner}/R_{outer} > 1$	56	39	22	9	5	5	4
χ^2 Statistic	4.9	4.1	6.2	4.8	1.7	0.69	0.4
χ^2 Probability	0.03	0.04	0.01	0.03	0.20	0.40	0.50
Fraction $R_{inner}/R_{outer} < 1$	0.594	0.602	0.656	0.700	0.667	0.615	0.600
Lower 1σ Confidence	0.046	0.055	0.069	0.106	0.162	0.141	0.204
Upper 1σ Confidence	0.044	0.053	0.064	0.091	0.135	0.172	0.180